Development of Mixers for the High-Resolution Spectrometer of the Millimetron Space Observatory

Ivan V. Tretyakov, Andrey V. Khudchenko, Kirill I. Rudakov, Irina V. Ivashentseva, Natalia S. Kaurova, Boris M. Voronov, Maria S. Kirsanova, Tatiana I. Larchenkova, Gregory N. Goltsman, Andrey M. Baryshev, Ronald Hesper, Fedor V. Khan, Elena S. Zhukova, Artem M. Chekushkin, A. V. Melentev, K. V. Zhivetev, A. V. Terentiev, Valery P. Koshelets, *Senior Member, IEEE*, and S. F. Likhachev

***Abstract*—The study of the origin and transport of water in the universe is an important part of the scientific program of the Millimetron space observatory. This will be made possible by observations conducted in single-dish mode using an onboard instrument—the high-resolution spectrometer (HRS). This instrument incorporates heterodyne array receivers operating within the range $0.5-2.7$ THz, comprising 3-pixel arrays of superconductor–insulator–superconductor mixers operating at frequencies below 1.3 THz and 7-pixel matrix receivers based on NbN HEB mixers observing above 1.3 THz. This article presents the current status of development for a mixers planned for use in the HRS instrument of the Millimetron space observatory.**

***Index Terms*—Heterodyne receiver, matrix of detectors, NbN thin film, THz range.**

I. Introduction

THE study of cosmic objects and processes in the Universe carried out from the surface of the Earth is limited by the atmosphere of the planet. In the submillimeter range 0.02–1 mm absorption is due to molecules of water vapor H_2O, carbon dioxide CO_2, and oxygen O_2. The H_2O molecule is the most important molecule for studying the evolution of life in the Universe. However, atmospheric water vapor makes it difficult to ground-based observations of the H_2O emission from space objects. The deployment of space observatories equipped with broadband and sensitive receivers make it possible to study many water emission lines including the most important ground-state ones. Therefore, such space observatories make it possible to study water abundances and the entire chain of water transformations in the interstellar medium (ISM) from dense clouds to protoplanetary disks.

The study of the origin and transport of water in the Universe ("water" program hereafter) is an important part of the scientific program of the Millimetron space observatory presented by [1], [2], [3]. The Millimetron is a space telescope with a cooled 10-m mirror designed to study various objects in the Universe in the millimeter and sub-mm bands. The "water" program has two main goals. The first goal is to determine the abundance of water and chemically related species in various space objects from galaxies to comets. The abundances help to study the mechanisms of water formation in the gas phase and on the surface of interstellar dust and check a hypothesis that water ice is the main reservoir of this molecule in the ISM. If the water ice is indeed the main reservoir, it is crucial to understand how molecules appear in the gas phase and reveal the most important desorption process in particular conditions in the ISM. Previous observations of the water emission lines by *Herschel* showed that water is also formed in the regions where shock waves compress and heat the ISM, see e.g., [4]. Accordingly, the Millimetron telescope will focus on the study of shocked gas and dust in regions of active star formation within our Galaxy and beyond. The second goal of the "water" program is to investigate the transport of water between different types of space objects and the link between interstellar water molecules and the emergence of life on Earth. This part of the observational program will include protoplanetary disks and comets where ices from the parental molecular cloud could survive. These studies will be performed in order to compare the water on the Earth with the interstellar molecules in terms of the abundances of deuterated molecules. For a more detailed overview of the specific aims of this research, please see [5]. Ambitious goals of the Millimetron telescope require high sensitivity about 20–100 mK for water and 5–10 mK for the lines of deuterated water with high spectral resolution up to 0.1–0.3 km s^{-1}.

Received 20 July 2024; revised 20 October 2024; accepted 11 November 2024. Date of publication 25 November 2024; date of current version 5 March 2025. This work was supported in part by the Russian Science Foundation under Project 23-12-00187 and in part by the Ministry of Science and Higher Education of the Russian Federation through SIS mixers development under Agreement 075-15-2024-538. *(Corresponding author: Ivan V. Tretyakov.)*

Ivan V. Tretyakov, Andrey V. Khudchenko, Kirill I. Rudakov, Tatiana I. Larchenkova, and S. F. Likhachev are with the Astro Space Center of P.N. Lebedev Physical Institute, Russian Academy of Science, 119991 Moscow, Russia (e-mail: tretyakov@asc.rssi.ru).

Irina V. Ivashentseva, Natalia S. Kaurova, Boris M. Voronov, and Gregory N. Goltsman are with the Moscow State University of Education, 119435 Moscow, Russia.

Maria S. Kirsanova is with the Astro Space Center of P.N. Lebedev Physical Institute, Russian Academy of Science, 119991 Moscow, Russia, and also with the Institute of Astronomy, Russian Academy of Sciences, 119017 Moscow, Russia.

Andrey M. Baryshev and Ronald Hesper are with the Kapteyn Astronomical Institute, University of Groningen, 9747 AD Groningen, The Netherlands (e-mail: a.m.baryshev@astro.rug.nl).

Fedor V. Khan, Artem M. Chekushkin, and Valery P. Koshelets are with the Kotel'nikov Institute, Radioengineering and Electronics RAS, 125009 Moscow, Russia (e-mail: valery@hitech.cplire.ru).

Elena S. Zhukova, A. V. Melentev, K. V. Zhivetev, and A. V. Terentiev are with the Moscow Institute of Physics and Technology, National Research University, 141700 Dolgoprudny, Russia.

Color versions of one or more figures in this article are available at https://doi.org/10.1109/TTHZ.2024.3505592.

Digital Object Identifier 10.1109/TTHZ.2024.3505592

2156-342X © 2024 IEEE. All rights reserved, including rights for text and data mining, and training of artificial intelligence and similar technologies. Personal use is permitted, but republication/redistribution requires IEEE permission. See https://www.ieee.org/publications/rights/index.html for more information.

Authorized licensed use limited to: Kotel'nikov Inst of Radio Eng & Electronics - RAS. Downloaded on April 18,2025 at 13:46:57 UTC from IEEE Xplore. Restrictions apply.

TABLE I
FREQUENCY RANGES AND MAIN PARAMETERS OF HRS INSTRUMENT RECEIVERS

Chanal	Band (GHz)	Pixel	Technology	T_n (K)	Res. (")
$M1$	500–600	3	SIS	200	14
$M2$	740–900	3	SIS	400	9
$M3$	1080–1230	3	SIS	1000	7
$M4$	$1300-1400$	7	HEB	1000	6
$M5$	$1890-1910$	7	HEB	1200	4
$M6$	$2390-2410$	7	HEB	1400	3
$M7$	$2660-2680$	7	HEB	1400	3

II. HIGH-RESOLUTION SPECTROMETER (HRS) GENERAL DESCRIPTION

As part of Millimetron "water" program, observations will be made in single-dish mode in the following frequency ranges: 500–600, 740–900, 1080–1230, 1300–1400, 1890–1910, 2390–2410, and 2660–2680 GHz using heterodyne instrument HRS. The spectral lines located within these frequency bands, along with the scientific rationale for their observation, are described in details in [5]. The main technical parameters of the spectrometer are presented in Table I. For the first three bands it is planned to use 3-pixel receivers based on superconductor–insulator–superconductor (SIS) mixers. The intermediate frequency (IF) band is assumed to be $4-12$ GHz. At the same time, it can be reduced to $4-8$ GHz to save onboard resources; such a reduction will not have a critical impact on scientific tasks. At frequencies above 1300 GHz, it is proposed to use a 7-pixel DSB receivers with H/V polarization based on hot-electron bolometers (HEBs) [6], [7]. The expected single-sideband noise temperature is presented in the penultimate column. Further in this article we will discuss in depth technical details regarding the mixers, with a view to elucidating the rationale behind the selected sensitivity. The final column in Table I depicts the projected angular resolution that can be achieved by an instrument for a 10-m primary mirror of the Millimetron observatory.

The preliminary design of the HRS for Millimetron space observatory [8] is a logical continuation of the HiFi instrument [9]. The difference is in focus on facilitating mapping capabilities through the configuration of compact arrays and by implementing the scanning regime for the HRS pickup mirror. The scanning mirror will be situated within the cold instrument container at a temperature of 20 K, in the focal area of the Millimtron Cassegrain optical system. It will facilitate the mapping of compact objects with dimensions within 20×20 arc minutes on the sky. It is proposed that the triangular 3-pixel configuration for the lower bands and hexagonal 7-pixel structure for the higher bands be implemented in order to enhance the mapping speed and mitigate the risks associated with potential mixer degradation. The reduction in the number of pixels for the bands with longer wavelengths is a consequence of the necessity to accommodate the wider beams. The higher number of pixels is not a primary consideration due to the rapid increase in the complexity of the instrument and the need for greater cooling power on board.

III. SIS MIXER-BASED HETERODYNE RECEIVERS

Terahertz receivers based on SIS mixers are known to be the most sensitive heterodyne instruments for frequency range roughly 200–1300 GHz [10]. The principal advantages of SIS mixers are their minimal local oscillator (LO) power requirements and their exceptionally low intrinsic noise. The noise temperature of the mixer in double sideband (DSB) mode is limited by the quantum value $hf/2k_B$ [11], [12], where h and k_B are the Planck and Boltzmann constants, respectively. This is why SIS mixers are already successfully used both for ground-based radio telescopes [13], [14], [15], [16], [17], and for space missions [9], [18].

A. 500–600 GHz Channel

This frequency range is well developed; SIS receivers have been implemented in space [9], [19] and at the largest ground-based multielement interferometer ALMA [20]. The new SEPIA Instrument was installed and commissioned at the Atacama Pathfinder Experiment telescope (APEX) [21] and equipped with a sideband separating SIS receiver operating operating between 578 and 738 GHz [22], [23].

For this mixer we follow the common approach of SIS junction been incorporated into Nb thin film structures manufactured on a quartz substrate. To cover the entire band 500–600 GHz we manufactured SIS junctions with a high current density. Due to the limitations of Al_2O_3 barrier technology, which provides current density only order of 10 kA/cm^2 without a critical deterioration in the quality of SIS junctions, we developed the fabrication of Nb-Al/AlN-NbN tunnel SIS junctions with a high tunnel barrier transparency, made by nitridization of the Al surface in an RF plasma discharge. In this configuration, niobium nitride is employed as the top electrode instead of pure niobium. The implementation of such structures not only increases the tunneling current density but also significantly elevates the total gap voltage of the junction, from 2.8 mV to a level reaching 3.7 mV. In addition, at high current densities for Nb-AlN-NbN junctions, the quality parameter, determined by the ratio of the subgap resistance to the normal one, R_j/R_n, turns out to be noticeably higher than for purely niobium junctions. The R_j/R_n value reaches 20 at a tunnel current density of 70 kA/cm^2, which indicates the high quality of the tunnel barrier [24]. However, to ensure good matching between these high-current-density junctions and the antenna, the use of submicron SIS junctions is required. One of our recent results is illustrated in Fig. 1, which depicts a 0.65 μm^2 size SIS junction demonstrating resistance of 23.7 Ohm, high quality factor R_j/R_n approaching 24, the gap voltage V_g close to 3.5 mV, and the current density is around 13 kA/cm^2. Implementation of the SIS junctions with AlN barrier is known to allow not only the realization of DSB noise temperature well below 100 K at frequencies up to 650 GHz, but also provide a very flat IF response from 4 to 12 GHz for heterodyne waveguide receiver [20]. Our mixer development is still ongoing, but based on the achieved sensitivities for similar mixers we put in the Table I expected single-sideband noise temperature of 200 K. This estimation is conservative in light of recent state-of-the-art results, which demonstrate a DSB noise temperature of approximately 60 K in the required frequency

Authorized licensed use limited to: Kotel'nikov Inst of Radio Eng & Electronics - RAS. Downloaded on April 18,2025 at 13:46:57 UTC from IEEE Xplore. Restrictions apply.

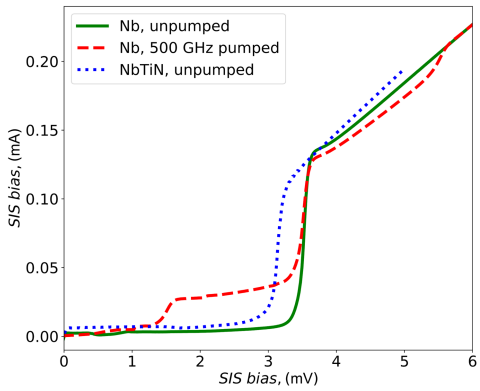

Fig. 1. *I-V* curves of Nb/Al-AlN/NbN SIS mixers: autonomous SIS junction with Nb bottom wiring for the embedding circuit—solid line; same junction pumped by 500 GHz radiation—dashed line; autonomous SIS junction with NbTiN bottom wiring for the embedding circuit—dotted line.

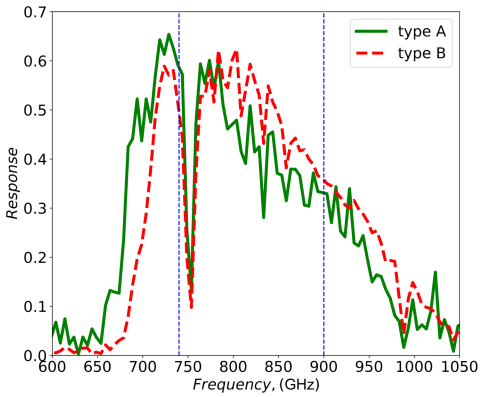

Fig. 2. Frequency responses of SIS mixers for design "A" and "B" measured using a Fourier transform spectrometer. The vertical dotted lines mark the band required for HRS.

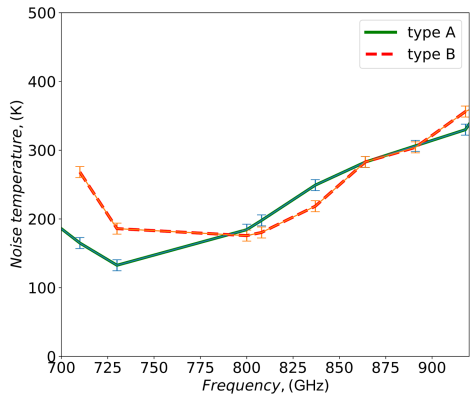

Fig. 3. SIS mixer noise temperatures for type "A" and type "B" designs measured by standard two-load (77 K/300 K) technique. The experimental data are corrected for the 88% transparent 12 μm mylar beam splitter used for the LO injection.

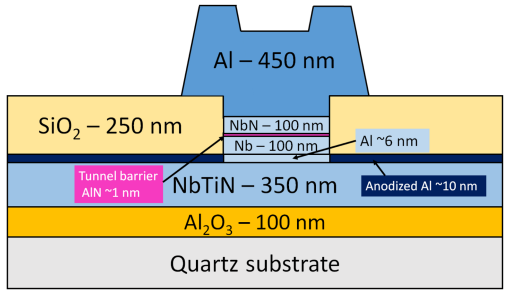

Fig. 4. Structure of the technological layers near Nb/Al-AlN/NbN junction embedded into NbTiN/Al microstrip line in the SIS mixer.

range [25]. This evidence suggests the potential for improving upon the expected number. In addition, we propose the utilization of a sideband-separating SIS mixer [22], [26] to facilitate in-flight sideband calibration, with the objective of populating at least one pixel.

B. 740–900 GHz Channel

For the frequency range 740–900 GHz we plan to build our instrument based on heritage gained during developed of the SIS mixer for CHAMP+ instrument for APEX telescope [27], [28]. The intended frequency range for that receiver was within the $787-950$ GHz atmospheric window, however, the mixer response is high also at frequencies down to 700 GHz for two types of the designs, see Fig. 2. The figure shows typical frequency responses for twin-junction mixers of those two types. The responses are presented in a broader range to demonstrate that the coupling is almost perfect for the intended HRS band. The DSB noise temperature measured for one of the most sensitive SIS mixers form those two types is illustrated in Fig. 3. In the target frequency range it is approximately 200 K.

Currently we develop an SIS mixer based on high critical current density Nb-AlN-NbN tunnel junctions embedded in a microstrip line consisting of 350 nm thick NbTiN bottom electrode (ground plane) and 480 nm thick Al top electrode. Microstrip electrodes are separated by an insulating layer of SiO_2 250 nm thick. The SIS junction is located on the NbTiN film, and the top NbN layer is in contact with the top Al electrode (see cross-section in Fig. 4). The *I-V* curve for a recently fabricated SIS junction is illustrated in Fig. 1 by a dotted line. The junction has an area of about 0.35 μm^2 (see Fig. 5), a current density of 28 kA/cm^2, a normal resistance of 21 Ohm, and a gap voltage V_g of 3.13 mV due to the high transparency of the AlN tunnel barrier. The quality factor R_j/R_n remains relatively high at approximately 14. The NbTiN film has been chosen because of high energy gap and the thickness is taken to exceed the expected London penetration depth. The NbN top electrode enhances the potential for operation of such structures at high frequencies (above 700 GHz), when the size of the photon step is hf/e exceeds V_g [29], [30]. In addition to the two demonstrated twin-junction mixer designs, we develop modified versions and a single-junction option, optimized for the target band. Fig. 2 illustrates one of the test mixers, which includes an SIS junction embedded in a microstrip line.

Similar to the $500-600$ GHz instrument we plan to use here at least one sideband-separating pixel. This will be based on the experience gained in the development of $800-950$ GHz two-sideband SIS mixer [31].

Authorized licensed use limited to: Kotel'nikov Inst of Radio Eng & Electronics - RAS. Downloaded on April 18,2025 at 13:46:57 UTC from IEEE Xplore. Restrictions apply.

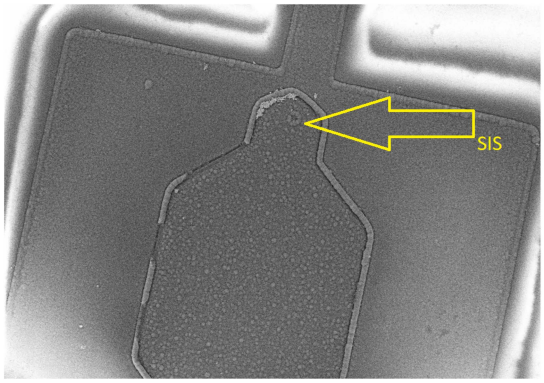

Fig. 5. E-beam photo of the test mixer structure near Nb/Al-AlN/NbN junction embedded into NbTiN/Al microstrip line in the SIS-receiver.

C. 1080–1230 GHz Channel

This is the highest frequency band in HPS instrument based on SIS mixer technology. In the past it was successfully proven for HiFi Band 4 and Band 5 [9], [32]. The DSB noise temperature for HiFi Band 4 was below 400 K for frequencies up to 1120 GHz. This indicates that it may be possible to reach the SSB noise temperature of approximately 1000 K with this receiver.

We plan to build our SIS mixer using the same technology as for the band 740–900 GHz, i.e. based on Nb-AlN-NbN junctions and with NbTiN ground electrode. To ensure the feasibility of superconducting mixer based on NbTiN within the specified frequency range, we have addressed separately the question on the quality of the produced NbTiN films at frequencies up to 1300 GHz.

We have already started the work on studying the superconducting NbTiN films, which would allow us to manufacture the devices with operating frequency range up to 1.2 THz [33], [34]. The fabricated films were measured using terahertz time-domain spectrometer Menlo Systems Tera K15. In [33], we have found the optimal pressure of nitrogen in magnetron for obtaining the NbTiN film on silicon substrate with high energy gap Δ, critical temperature T_c, and low normal-state resistivity near T_c. In [34] we studied the impact of the layers which are necessary for technological processes (buffer 100 nm-thick Al_2O_3 layer at the substrate for the surface protection in RIE-processes; 10 nm-thick anodized Al layer for protection of the bottom electrode during etching in CF_4 when SIS-junctions are formed). Only slight deterioration of the NbTiN film properties was observed for all the buffer layers. Here, we studied the properties of NbTiN films sputtered on quartz substrates.

Our results show that NbTiN film with gap frequency as high as 40 cm^{-1} or 1200 GHz can be obtained, which corresponds to $hf_{gap} = 2\Delta = 4.82$ meV. Fig. 6 depicts the spectra of transmission coefficient (a), permittivity (b) and real part of conductivity (c) for the NbTiN film on quartz substrate with Al $_2$ O_3 buffer layer and anodized Al on the film surface. This is exactly the film that forms bottom electrode in superconductor microstrip line in receiver (see Fig. 4).

The described mixer technology demonstrates the noise temperature level of approximately 200 K at a frequency of 800 GHz.

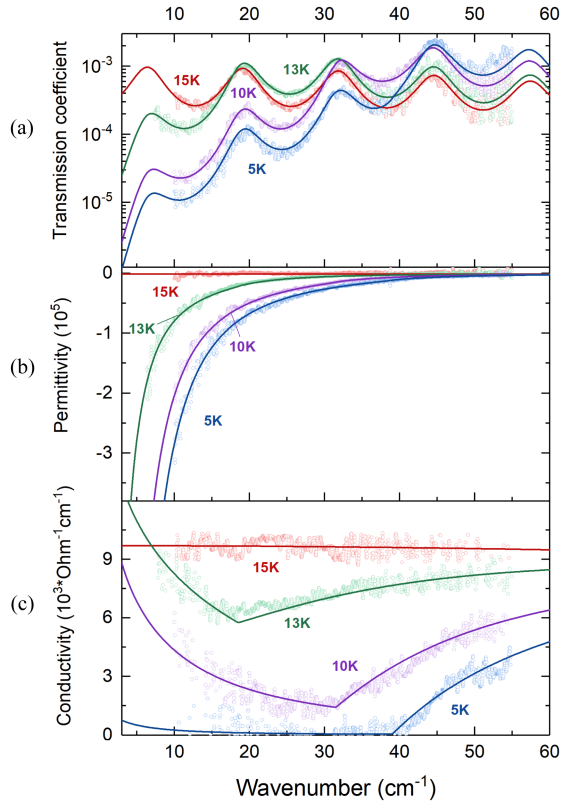

Fig. 6. Measured spectra of the transmission coefficient (a), permittivity (b), and conductivity (c) of the superconducting NbTiN film on quartz substrate with 100 nm Al_2O_3 buffer layer and anodized aluminum on surface.

At a frequency of 1200 GHz, we anticipate twofold increases in losses in NbTiN due to the film's twice higher real part, as indicated by simulations. In addition, the Al film will operate in an anomalous skin effect regime, as referenced in [35] and [36], as a result the bulk conductivity σ varies as a $1/f^{1/3}$ and increases only by a factor of 1.15. Furthermore, the SIS mixer quantum noise scales linearly with frequency, and only a factor of 1.5 increase is expected. Based on these observations, the factor of 2–2.5 increase in the final mixer noise temperature is a realistic estimation. The results obtained thus far instill confidence that the embedding circuit for the future 1080–1230 GHz SIS mixer will exhibit acceptable losses, thereby enabling the desired receiver noise temperature to be achieved.

IV. HEB Mixer-Based Heterodyne Receivers

The high sensitivity of HEB mixers ensured their application in joint NASA and DLR astronomical project : SOFIA airborne observatory with a 2.5-m mirror capable of observing at frequencies from 1 to 5 THz. [37] and TELIS [38] for operation in the range 1.76–1.86 THz. In the HERSCHEL space observatory, the 1.4–1.9 THz channel also used HEB mixers [9]. Among the SOFIA instruments, the 1.4, 1.9, and 2.5 THz channels of the GREAT instrument are based on single waveguide NbN HEB mixers [39]. The upGREAT tool, the successor to GREAT, is already a multipixel heterodyne matrix [40]. The upGREAT low-frequency array (LFA) consists of 2 × 7 pixel waveguide

Authorized licensed use limited to: Kotel'nikov Inst of Radio Eng & Electronics - RAS. Downloaded on April 18,2025 at 13:46:57 UTC from IEEE Xplore. Restrictions apply.

HEBs, two sets needed to separate polarizations at 1.9–2.5 THz. The upGREAT high-frequency array (HFA) consists of seven waveguide HEBs tuned to operate at 4.745 THz. The hexagonal configuration is chosen for maximum display efficiency. An LFA with a noise temperature of 600 K at the center of the frequency range was successfully commissioned to observe the [C II] line at 1.905 THz. Direct detection of atomic oxygen on the dayside and nightside of Venus [41] was demonstrated by HFA. Such balloon-based instruments as STO, STO-2, GUSTO, and OSAS-B also used NbN HEB mixers [42], [43], [44], [45]. The DOME A observatory, being developed by the Purple Mountain Observatory of the Chinese Academy of Sciences, may become the most promising ground-based observation platform for THz astronomy [46]. It is planned to build a 5-m THz telescope, DATE5, equipped with a dual-band heterodyne receiver for atmospheric window frequencies of 0.85 and 1.4 THz based on an HEB mixers.

A disordered ultrathin ($3.5-4$ nm) superconducting NbN film is used as a sensitive element in these terahertz range HEB mixers. Due to the physical principle of the HEB mixer operation, this "ingredient" is the most crucial, the combination of extremely low film thickness and its superconducting properties determines the characteristics of the final receiver.

Modern NbN HEBs as heterodyne detectors have almost reached their sensitivity limit (quantum limit $hf/2k_B$) [39], [47], [48], however, they have a conversion band (IF band) not exceeding $3-4$ GHz [49]. Further reduction of the noise temperature, an increase in the IF band as well as reduction of the required LO power has a significant practical interest. Currently, each pixel of the heterodyne matrix—HEB mixer—is considered as a separate detector, requiring individual adjustment of the bias voltage and the LO power. With a matrix size of at least a ten pixels, such an individual approach is difficulty applicable. The solution of the problem could be the fabrication of an unified HEB mixers that do not require individual settings. To meet the issue we improve the technology for deposition of NbN films and the NbN HEB mixers fabrication processes to fabricate mixers with as close as possible $R(T)$ characteristics and a minimum spread of normal resistances R_{300} for devices with the same geometry within the same batch.

A. NbN HEB Mixers Fabrication and DC Test

The HEB mixers were fabricated from a bilayer NbN-Au structure with a thickness of NbN film of $3.5-4$ and Au $20-25$ nm deposited *in-situ* using reactive magnetron sputtering onto the surface of a high-resistivity Si substrate. The substrate temperature could vary up to $900\,^{\circ}$C. Before film deposition, the substrate surface was cleaned in oxygen plasma, followed by treatment in a hydrofluoric acid solution. This, along with speed optimization by reducing the discharge current to $300\,\mu$A, made it possible to achieve high uniformity of the superconducting properties (film thickness, T_c and surface resistance R_s) of the NbN film over the Si substrate surface.

The dependence of the critical temperature and surface resistance of NbN films at a deposition time of 5 s is presented in Fig. 7. The optimal values of the critical temperature T_c

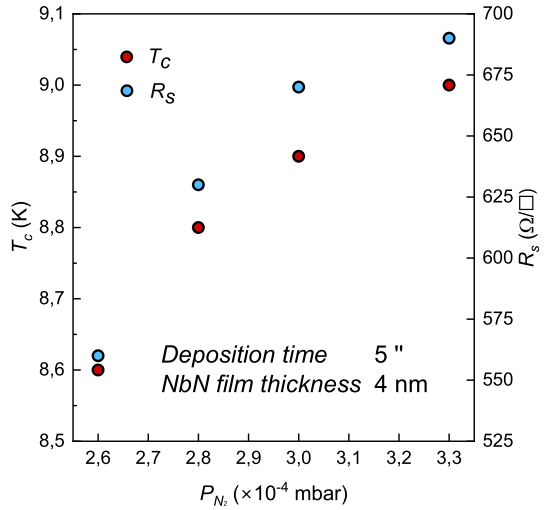

Fig. 7. Dependence of the T_c and R_s of the NbN films on the N_2 partial pressure during deposition process, each deposition took 5 s.

and critical current density j_c were obtained with the following parameters of the NbN film deposition process: substrate temperature $800-850\,^{\circ}$C, partial pressures of Ar and N_2 were $5-5.8\times10^{-3}$ and $3-3.3\times10^{-4}$ mbar, current and discharge voltage were $300\,\mu$A and 300 V. NbN deposition was followed by *in-situ* deposition of an Au layer after cooling the Si substrate down to $350\,^{\circ}\text{C}-400\,^{\circ}$C. Long time cooling of the Si substrate made it possible to anneal the fabricated NbN film to improve its superconducting properties and its distribution over the substrate. The NbN film deposition rate, for given process characteristics, was determined by test the dependence of film thickness on sputtering time. Same to the NbN films, the Au layer thickness was controlled over the deposition process time based on the obtained deposition rates. The thickness of the deposited NbN films was controlled using an atomic force microscope AFM.

In the process of an HEB mixer fabrication, electron and photo lithography methods, chemical and ion etching processes, thermal metal deposition and electron beam evaporation deposition, as well as the lift off process in acetone are used. For photo and electron lithography processes, Ti/Au alignment marks are made on top of the Au surface of the NbN/Au two-layer structure. This is followed by the fabrication of the spiral THz antenna and setting the width W of the future NbN mixer bridge using electron lithography and liquid and plasma-chemical etching processes. The photolithography method, thermal deposition of Ti and Au layers and the lift off process are used to form the outer part of the antenna and the mixer bond pads. At the final step of the fabrication, the length L of the NbN bridge of the mixer is set; for this purpose, electron lithography, ion and liquid etching methods are used. Central part of the mixer is covered with a layer of SiO_2 to prevent the external undesirable environment influence.

Typical sizes of superconducting bridges of HEB mixers ranged from $0.1--0.4\,\mu$m in length L, and $1--4\,\mu$m in width W. The SEM photo and sketched cross-section of the central part of the THz antenna, shown in Fig. 8. With a normal

Authorized licensed use limited to: Kotel'nikov Inst of Radio Eng & Electronics - RAS. Downloaded on April 18,2025 at 13:46:57 UTC from IEEE Xplore. Restrictions apply.

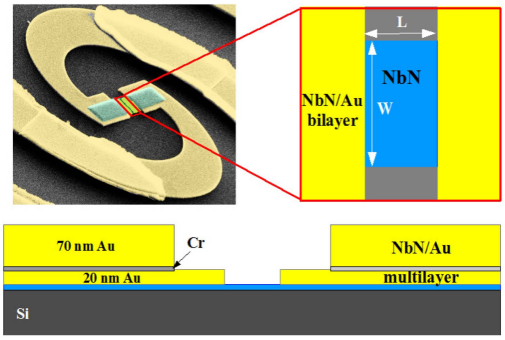

Fig. 8. False color SEM photo and cross-section sketch of central part of a typical NbN HEB device, showing the active material of NbN (blue). The yellow parts made of gold (Au) serve as ports of THz spiral antenna.

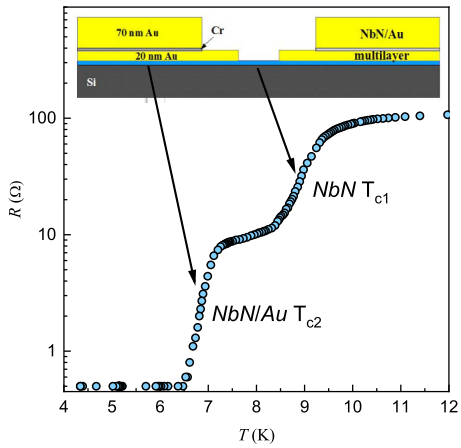

Fig. 9. Temperature dependence of the NbN HEB mixer resistance R. The appearance of the second superconducting transition at T_{c2} is caused by the proximity effect in the NbN film under *in-situ* Au. The value of the mixer resistance after the first transition is determined by the width NbN of the bridge and the coherence length ξ in the NbN film. Resistance appears in a superconducting NbN film due to the process of conversion of normal electrons into Cooper pairs. The conversion region is determined by the coherence length of the resulting Cooper pairs.

resistance per square NbN film $R = 650 - 700\,\Omega/\square$ (with a NbN thickness of $3.5 - 4$ nm), the ratio of the bolometer length to its width L/W is kept constant to achieve a $65\,\Omega$ resistance in the normal state for optimal RF and IF coupling.

Optimized sequence of the HEB mixers fabrication processes, the sensitive element—the NbN bridge of the mixer—during the fabrication had been coated with *in-situ* Au layer, made it possible to minimize the spread of normal resistances R_{300} of the mixer; along with the optimized process of NbN film deposition, it also allowed to minimize the spread in T_c down to 0.1 K for mixers fabricated within the same process. The dependence of the NbN HEB mixers resistance R as function of the temperature is presented in Fig. 9. A conventional HEB device consists of two main parts. The central, bare NbN film with critical temperature T_{c1}, connected to a superconducting NbN-Au layer, with critical temperature T_{c2}, which serves as THz antenna ports. The appearance of the second superconducting transition at T_{c2} is caused by the suppression of superconductivity in the NbN film under and near of the thin *in-situ* Au due to the proximity effect. The remaining NbN film under the shunt thick Au antenna

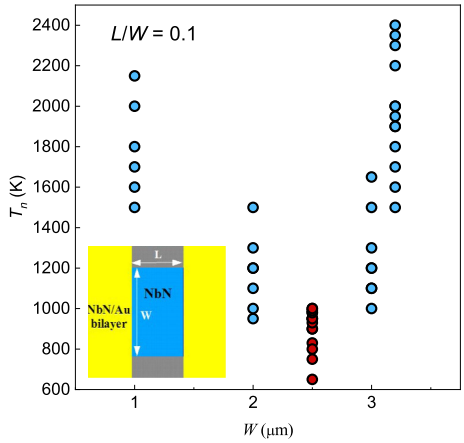

Fig. 10. NbN HEB mixer DSB noise temperature T_n as function of the NbN bridge width W measured at 2.52 THz LO frequency. The results of measuring the $T_n{}^{\mathrm{DSB}}$ for two types of NbN HEB mixers. The red circles indicate the results for mixers fabricated using the new technology. The blue circles indicate the $T_n{}^{\mathrm{DSB}}$ results for mixers fabricated using the technology presented in [48].

is in a fully normal state at temperatures above 4.2 K. The difference in T_c between the NbN bridge and NbN/Au bilayer for our case exceeds 2 K. It indirectly indicates the quality of the electrical contact, as well as the thickness of the NbN film. The proximity effect appears at sizes on the order of the coherence length ξ in a superconductor, which is on the order of 3 nm for thin NbN films.

B. NbN HEB Mixers Noise Temperature

DSB noise temperature $T_n{}^{\mathrm{DSB}}$ measurements were carried out at an LO frequency of 2.52 THz using the "cold" / "hot" (77 K/300 K) blackbody technique. A quantum cascade laser QCL was used as an LO source. QCL had an output power of about 5 mW, frequency tuning of about 10 GHz, power dissipation of 1 W at a physical temperature of 17 K. To couple the mixer with the radiation, we used an elliptical Si lens. Using a 3.5 μm-thick Mylar beamsplitter, the LO was combined with the blackbody. The transmittance of the beamsplitter was no less than 0.97 at a frequency of 2.52 THz. The optical window of the cryostat was made of high-density polyethylene HDPE. To prevent the direct detection effect, we used a cooled to 4 K narrow-band interference filter (about 200 GHz band) with a transmittance of 0.9. The cold amplifier with a gain of 35 dB had a T_n of no higher than 10 K in the $1 - 8$ GHz band. The cold amplifier have no microwave isolator. The U factor in the experiment was about 8–10 times. The estimated contribution of the optical path to the measured $T_n{}^{\mathrm{DSB}}$ value did not exceed 100 K. Fig. 10 shows the results of measuring the $T_n{}^{\mathrm{DSB}}$ for two types of NbN HEB mixers. The red circles indicate the results for mixers fabricated using the new technology. The NbN film deposition technology optimized the deposition rate (discharge current), nitrogen partial pressure, temperature substrates, and temporary cooling (annealing of the deposited film) to obtain uniform superconducting properties of the film at $3 - 4$ nm across Si wafer. In addition, changes were made to the mixer fabrication sequence—making a gap in *in-situ* Au for the NbN

Authorized licensed use limited to: Kotel'nikov Inst of Radio Eng & Electronics - RAS. Downloaded on April 18,2025 at 13:46:57 UTC from IEEE Xplore. Restrictions apply.

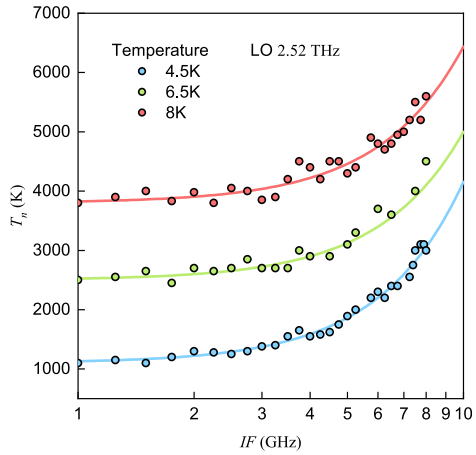

Fig. 11. NbN HEB mixer DSB T_n @2.52 THz as function of the IF measured on different bath temperature T.

mixer's bridge and adding wet acid instead ion etching etching at the final fabrication stage to reduce the spread in $R(T)$ curves of the mixers. The blue circles indicate the ${T_n}^{\mathrm{DSB}}$ results for mixers fabricated using the technology presented in [48]. The spread in ${T_n}^{\mathrm{DSB}}$ for mixers fabricated using optimized technology does not exceed 200 K with an average level of 800 K. This value well meets the design requirements and has a margin for losses in the future optical path of the instrument. Fig. 11 shows the experimental results of ${T_n}^{\mathrm{DSB}}$ in the IF band. The measurements were carried out for three temperatures 4 K, 6.5 K, and 8.5 K. Since the measurements were limited to the band of the cooled amplifier, the experimental points were approximated by a curve of the form ${T_n}^{\mathrm{DSB}}(f) = [1 + (f/\Delta f)]^2$ to determine the frequency Δf at which ${T_n}^{\mathrm{DSB}}$ will double. During the work, it was determined that as the temperature of the NbN HEB mixer increases, ${T_n}^{\mathrm{DSB}}$ naturally increases, but at the same time Δf also increases. This effect is caused by the design of the mixer, namely the presence in the mixer NbN bridge regions near the normal metal contacts of the antenna with suppressed superconductivity due to the proximity effect. Electron conversion regions at temperatures below T_{c2} block the diffusion of "hot" electrons into "cold" metal contacts.

V. Conclusion

The development of mixers, which can be used to build receivers for the HRS for Millimetron space observatory gives us confidence to formulate the expected sensitivity levels for all the bands within the the range $0.5 - 2.6$ THz. For channel $M1$ the Nb base SIS mixers with AlN tunnel barrier will be utilized. For channels $M2$ and $M3$ SIS mixers with NbTiN wiring will be built. To implement channels $M4 - M7$ the NbN HEB mixers will be used; the achieved unification of the parameters of the fabricated mixers will make it possible to create a heterodyne matrix of 7 pixels with parameters that meet the requirements of the instrument. Since the mixers use a logarithmic spiral antenna that works well in the $1 - 3$ THz band, it will be possible to use a pair (H/V polarization) of such matrices for sequential observation in channels $M4 - M7$.

References

[1] N. S. Kardashev et al., "Review of scientific topics for the millimetron space observatory," *Phys. Uspekhi*, vol. 57, no. 12, pp. 1199–1228, Dec. 2014.

[2] I. D. Novikov et al., "Objectives of the millimetron space observatory science program and technical capabilities of its realization," *Phys. Uspekhi*, vol. 64, no. 4, pp. 386–419, Jul. 2021.

[3] S. F. Likhahev and T. I. Larchenkova, "From the spektr-R project to the spektr-M project: Milestones in space radio astronomy," *Phys. Uspekhi*, vol. 67, no. 8, pp. 768–778, 2024.

[4] E. F. Van Dishoeck et al., "Water in star-forming regions: Physics and chemistry from clouds to disks as probed by Herschel spectroscopy," *Astron. Astrophys.*, vol. 648, Apr. 2021, Art. no. A24.

[5] M. S. Kirsanova et al., "The origin and transfer of water in the universe," *Phys. Uspekhi*, accepted for publication.

[6] E. M. Gershenzon et al., "Millimeter and submillimeter wave range mixer based on electronic heating of superconducting films in the resistive state," *Sov. Phys. Supercond.*, vol. 3, pp. 1582–1597, 1990.

[7] D. Prober, "Superconducting terahertz mixer using a transition-edge microbolometer," *Appl. Phys. Lett.*, vol. 62, no. 17, pp. 2119–2121, 1993.

[8] "Millimetron observatory website," 2024. [Online]. Available: https://millimetron.ru/en/

[9] T. De Graauw et al., "The Herschel-Heterodyne instrument for the far-infrared (HiFi)," *Astron. Astrophys.*, vol. 518, 2010, Art. no. L6.

[10] J. Zmuidzinas and P. L. Richards, "Superconducting detectors and mixers for millimeter and submillimeter astrophysics," *Proc. IEEE*, vol. 92, no. 10, pp. 1597–1616, Oct. 2004.

[11] J. R. Tucker and M. J. Feldman, "Quantum detection at millimeter wavelengths," *Rev. Modern Phys.*, vol. 57, no. 4, 1985, Art. no. 1055.

[12] A. R. Kerr, M. J. Feldman, and S.-K. Pan, "Receiver noise temperature, the quantum noise limit, and the role of the zero-point fluctuations," in *Proc. 8th Int. Symp. Space Terahertz Technol.*, 1997, pp. 101–111.

[13] "Alma observatory website," 2024. [Online]. Available: https://www.almaobservatory.org/en/about-alma/

[14] "The NOEMA radio telescope website," 2024. [Online]. Available: https://www.cnrs.fr/en/press/european-radio-telescope-noema-reaches-full-power

[15] "The submillimeter array (SMA) website," 2024. [Online]. Available: https://lweb.cfa.harvard.edu/sma/index.html

[16] "Apex - Atacama pathfinder experiment telescope website," 2024. [Online]. Available: https://www.eso.org/public/teles-instr/apex/

[17] "Iram - the 30-meter telescope website," 2024. [Online]. Available: https://iram-institute.org/observatories/30-meter-telescope/

[18] "Herschel space observatory website," 2024. [Online]. Available: https://www.esa.int/ScienceExploration/SpaceScience/Herscheloverview

[19] Y. Delorme et al., "Space-qualified SIS mixers for herschel space observatory's HiFi band 1 instrument," in *Proc. 16th Int. Symp. Space Terahertz Technol.*, 2005, pp. 444–448.

[20] A. Baryshev et al., "The ALMA Band 9 receiver-design, construction, characterization, and first light," *Astron. Astrophys.*, vol. 577, 2015, Art. no. A129.

[21] V. Belitsky et al., "Sepia–A new single pixel receiver at the apex telescope," *Astron. Astrophys.*, vol. 612, 2018, Art. no. A23.

[22] R. Hesper, A. Khudchenko, A. M. Baryshev, J. Barkhof, and F. P. Mena, "A high-performance 650-GHz sideband-separating mixer–design and results," *IEEE Trans. THz Sci. Technol.*, vol. 7, no. 6, pp. 686–693, Nov. 2017.

[23] A. Hacar et al., "Apex-sepia660 early science: Gas at densities above 107 cm- 3 towards OMC-1," *Astron. Astrophys.*, vol. 644, 2020, Art. no. A133.

[24] M. Y. Torgashin et al., "Superconducting integrated receiver based on Nb-AlN-NbN-Nb circuits," *IEEE Trans. Appl. Supercond.*, vol. 17, no. 2, pp. 379–382, Jun. 2007.

[25] J. W. Kooi et al., "Quantum limited SIS receiver technology for the detection of water isotopologue emission from comets," *IEEE Trans. THz Sci. Technol.*, vol. 10, no. 6, pp. 569–582, Nov. 2020.

[26] R. Hesper, A. Khudchenko, A. M. Baryshev, J. Barkhof, and F. P. Mena, "A new high-performance sideband-separating mixer for 650 GHz," in *Proc. Soc. Photo- Opt. Instrum. Eng. Conf. Ser.*, vol. 9914, 2016, pp. 99140G-1–99140G-11.

[27] A. Khudchenko et al., "High-gap Nb-AlN-NbN SIS junctions for frequency band 790–950 GHz," *IEEE Trans. THz Sci. Technol.*, vol. 6, no. 1, pp. 127–132, Jan. 2016.

[28] K. I. Rudakov et al., "THz range low-noise SIS receivers for space and ground-based radio astronomy," *Appl. Sci.*, vol. 11, no. 21, 2021, Art. no. 10087.

Authorized licensed use limited to: Kotel'nikov Inst of Radio Eng & Electronics - RAS. Downloaded on April 18,2025 at 13:46:57 UTC from IEEE Xplore. Restrictions apply.

[29] M. Westig, S. Selig, K. Jacobs, T. Klapwijk, and C. Honingh, "Improved Nb SIS devices for heterodyne mixers between 700 GHz and 1.3 THz with NbTiN transmission lines using a normal metal energy relaxation layer," *J. Appl. Phys.*, vol. 114, no. 12, 2013, Art. no. 124504.
[30] A. Traini et al., "The influence of lo power heating of the tunnel junction on the performance of THz SIS mixers," *IEEE Trans. THz Sci. Technol.*, vol. 10, no. 6, pp. 721–730, Nov. 2020.
[31] A. Khudchenko et al., "Design and performance of a sideband separating SIS mixer for 800–950 GHz," *IEEE Trans. THz Sci. Technol.*, vol. 9, no. 6, pp. 532–539, Nov. 2019.
[32] A. Karpov et al., "Low noise 1 THz–1.4 THz mixers using Nb/Al-AlN/NbTiN SIS junctions," *IEEE Trans. Appl. Supercond.*, vol. 17, no. 2, pp. 343–346, Jun. 2007.
[33] F. V. Khan et al., "Characterization of microwave properties of superconducting NbTiN films using TDS," *IEEE Trans. THz Sci. Technol.*, vol. 13, no. 6, pp. 627–632, Nov. 2023.
[34] E. S. Zhukova et al., "Impact of the buffer layers and anodization on properties of NbTiN films for THz receivers," *IEEE Trans. Appl. Supercond.*, vol. 34, no. 3, May 2024, Art. no. 1100605.
[35] R. Finger and A. R. Kerr, "Microwave loss reduction in cryogenically cooled conductors," *Int. J. Infrared Millimeter Waves*, vol. 29, no. 10, pp. 924–932, 2008.
[36] A. B. Pippard, "The surface impedance of superconductors and normal metals at high frequencies. II. the anomalous skin effect in normal metals," *Proc. Roy. Soc.*, vol. A191, 1947, Art. no. 385.
[37] "Stratospheric observatory for infrared astronomy (sofia)," 2024. [Online]. Available: http://www.sofia.usra.edu
[38] R. W. M. Hoogeveen et al., "New cryogenic heterodyne techniques applied in TELIS: The balloonborne THz and submillimeter limb sounder for atmospheric research," in *Proc. Conf. SPIE Infrared Spaceborne Remote Sens. XI*, M. Strojnik, Ed., 2003, vol. 5152, pp. 347–355.
[39] P. Pütz et al., "Terahertz hot electron bolometer waveguide mixers for great," *Astron. Astrophys.*, vol. 542, 2012, Art. no. L2.
[40] C. Risacher et al., "First Supra-THz heterodyne array receivers for astronomy with the SOFIA observatory," *IEEE Trans. THz Sci. Technol.*, vol. 6, no. 2, pp. 199–211, Mar. 2016.
[41] H.-W. Hübers et al., "Direct detection of atomic oxygen on the dayside and nightside of venus," *Nature Commun.*, vol. 14, no. 1, 2023, Art. no. 6812.
[42] C. Walker et al., "The stratospheric terahertz observatory (STO): An LDB experiment to investigate the life cycle of the interstellar medium," in *Proc. 19th Int. Symp. Space Terahertz Technol.*, 2008, pp. 9–13.
[43] D. Hayton et al., "A 4.7 THz heterodyne receiver for a balloon borne telescope," in *Proc. SPIE Conf. Millimeter, Submillimeter, Far-Infrared Detectors Instrum. Astron. VII*, 2014, vol. 9153, pp. 583–589.
[44] C. Walker et al., "Gal/Xgal U/LDB Spectroscopic/Stratospheric THz observatory: GUSTO," in *Proc. Conf. SPIE Millimeter, Submillimeter, Far-Infrared Detectors Instrum. Astron. XI*, 2022, vol. 12190, Art. no. 121900E.
[45] M. Wienold et al., "OSAS-B: A balloon-borne terahertz spectrometer for atomic oxygen in the upper atmosphere," *IEEE Trans. THz Sci. Technol.*, vol. 14, no. 3, pp. 327–335, May 2024.
[46] S.-C. Shi et al., "Terahertz and far-infrared windows opened at dome a in antarctica," *Nature Astron.*, vol. 1, no. 1, 2017, Art. no. 0001.
[47] B. Mirzaei et al., "Reduced noise temperatures of a THz NbN hot electron bolometer mixer," *IEEE Trans. Terahertz Sci. Technol.*, early access, Oct. 7, 2024, doi: 10.1109/TTHZ.2024.3475010.
[48] I. Tretyakov et al., "Low noise and wide bandwidth of NbN hot-electron bolometer mixers," *Appl. Phys. Lett.*, vol. 98, no. 3, 2011, Art. no. 033507.
[49] J. J. Baselmans et al., "Doubling of sensitivity and bandwidth in phonon cooled hot electron bolometer mixers," *Appl. Phys. Lett.*, vol. 84, no. 11, pp. 1958–1960, 2004.

Ivan V. Tretyakov received the M.S. degree in solid state physics from Pomor State University, Arkhangelsk, Russia, in 2006, and the Ph.D. degree in radio physics from the Kotel'nikov Institute of Radio Engineering and Electronics, Russian Academy of Sciences, Moscow, Russia, in 2013.

Since 2006, he has been with the Moscow State Pedagogical University, Moscow, Russia. From 2020, he was with Astro Space Center, Lebedev Physical Institute, Russian Academy of Sciences. His research focuses on the development of THz and infrared devices.

Andrey V. Khudchenko received the M.S. degree in applied physics and mathematics and the Ph.D. degree in radiophysics from the Moscow Institute of Physics and Technology, Moscow, Russia, in 2007 and 2009, respectively.

From 2004 to 2008, he was an Engineer and, in 2009, a Researcher with the Kotel'nikov Institute of Radio Engineering and Electronics, Russian Academy of Sciences, Moscow. From 2010 to 2015, he was an Instrument Scientist with The Netherlands Institute for Space Research SRON, Leiden, The Netherlands. From 2015 to 2020, he was an Instrument Scientist with Kapteyn Astronomical Institute, University of Groningen, Groningen, The Netherlands. Since 2020, he has been with Astro Space Center, Lebedev Physical Institute, Russian Academy of Sciences. His research focuses on the development of new heterodyne THz instruments.

Kirill I. Rudakov received B.S. and M.S. degrees in applied physics and mathematics from the Moscow Institute of Physics and Technology, in 2013 and 2015, respectively. He is currently working toward the Ph.D. degree with Kapteyn Astronomical Institute, University of Groningen, Groningen, The Netherlands.

After internships as a Research Student in the ALPHA experiment with CERN in 2013 and as a Guest Scientist in the CHAMP+ experiment with SRON in 2014, he started a Ph.D. research with the Kapteyn Astronomical Institute, University of Groningen, Groningen, The Netherlands, in 2016. His Ph.D. research is devoted to the modeling and development of elements of the array SIS receivers in terahertz range. His research interests include heterodyne waveguide SIS-based receivers and high-frequency simulations of superconducting circuits, and measurements of them.

Irina V. Ivashentseva received the B.S. degree in fundamental physics (in english) from Moscow State Pedagogical University, Moscow, Russia, in 2023. She is currently working toward the master's degree in applied electronics and photonics with the National Research University Higher School of Economics, Moscow.

Since 2020, she has been a Research Assistant with the Laboratory of quantum detectors, Moscow State Pedagogical University, Moscow. The main subject of work is thin film sputtering and fabrication and characterization of HEB.

Natalia S. Kaurova, photograph and biography not available at the time of publication.

Boris M. Voronov, photograph and biography not available at the time of publication.

Maria S. Kirsanova received the M.S. degree in physics from Ural State University, Ekaterinburg, Russia, in 2005, and the Ph.D. degree in astronomy from the Institute of Astronomy, Russian Academy of Sciences, Moscow, Russia, in 2009.

Since 2005, she has been with the Institute of Astronomy of the Russian Academy of Sciences, where she is currently a Senior Researcher. Since 2023, she has been with Astro Space Center, Lebedev Physical Institute, Moscow. She is experienced in observations with mm and submm telescopes and in numerical modeling of interstellar medium.

Authorized licensed use limited to: Kotel'nikov Inst of Radio Eng & Electronics - RAS. Downloaded on April 18,2025 at 13:46:57 UTC from IEEE Xplore. Restrictions apply.

Tatiana I. Larchenkova received the M.S. degree in physics from Moscow Engineering Physics Institute, Moscow, Russia, in 1993, and the Ph.D. and D.Sc. (habilitation) degrees in astronomy from Lebedev Physical Institute, Russian Academy of Sciences, Moscow, Russia, in 2000 and 2021, respectively.

Since 1999, she has been with Lebedev Physical Institute, Russian Academy of Sciences, where she is currently the Head of the Department of Theoretical Astrophysics and Cosmology.

Gregory N. Goltsman, photograph and biography not available at the time of publication.

Andrey M. Baryshev received the master's degree (*summa cum laude*) in physical quantum electronics from the Moscow Institute of Physics and Technology, Moscow, Russia, in 1993, and the Ph.D. degree in physics from the Technical University of Delft, Delft, The Netherlands, in 2005.

He is currently a Senior Instrument Scientist. Since 1998, he has been with the SRON Low Energy Astrophysics Division and the Kapteyn Astronomical Institute, University of Groningen, Groningen, The Netherlands. Since 2000, he has been involved in a joint effort to develop the SIS receiver (600–720 GHz) for ALMA. In 2013, he became an Associate Professor of astronomical instrumentation for the far-infrared with Kapteyn Astronomical Institute, University of Groningen. His research interests include the areas of heterodyne and direct detectors for large focal plane arrays at THz frequencies, and quasioptical system design and experimental verification.

Dr. Baryshev was the recipient of a Netherlands Organisation for Scientific Research-VENI grant for research on heterodyne focal plane array technology in 2008, and an EU commission Starting Researcher Grant for work on direct detector focal plane arrays in 2009.

Ronald Hesper received the M.Sc. degree in experimental solid state physics from the University of Leiden, Leiden, The Netherlands, in 1994, and the Ph.D. degree in experimental solid state physics from the University of Groningen, Groningen, The Netherlands, in 2000.

He is currently involved in the development of new heterodyne detector technologies and industrialization of the ALMA Band 2 receivers. Since 2000, he has been an Instrument Scientist with Kapteyn Astronomical Institute, University of Groningen. From 2000 to 2008, he was involved in the technological development of the ALMA Band 9 receivers, including the process of industrialization, as well as related projects, such as the CHAMP+ mixer arrays for APEX; from 2008 to 2013, on the development of a sideband-separating mixer upgrade for the ALMA Band 9 receivers; and from 2013 to the beginning of 2015, on the industrialization of the ALMA Band 5 receivers.

Fedor V. Khan received the B.S. and M.S. degree in applied mathematics and physics from the Moscow Institute of Physics and Technology, Dolgoprudny, Russia, in 2021 and 2023, respectively, where he is currently working toward the Ph.D. degree in condensed matter physics.

Since 2019, he has been an Engineer with the Kotelnikov Institute of Radio Engineering and Electronics, Russian Academy of Sciences, Moscow, Russia, working on characterization of the superconducting materials for THz-range electronics and modeling of superconducting devices.

Elena S. Zhukova received the M.S. degree in applied physics and mathematics and the Ph.D. degree in condensed matter physics from the Moscow Institute of Physics and Technology, Moscow, Russia, in 2007 and 2010, respectively.

From 2010 to 2014, she was a Junior Researcher with A.M. Prokhorov General Physics Institute, Russian Academy of Sciences, Moscow. Since 2014, she has been a Senior Researcher and a Deputy Head of the Laboratory of Terahertz Spectroscopy, Moscow Institute of Physics and Technology (National research institute), Dolgoprudnyi, Russia. Her scientific interests include the field of terahertz and infrared spectroscopy of systems with correlated electronic states.

Artem M. Chekushkin, photograph and biography not available at the time of publication.

A. V. Melentev, photograph and biography not available at the time of publication.

K. V. Zhivetev, photograph and biography not available at the time of publication.

A. V. Terentiev, photograph and biography not available at the time of publication.

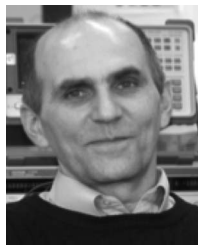

Valery P. Koshelets (Senior Member, IEEE) received the M.S. degree in physics from Lomonosov Moscow State University, Moscow, Russia, in 1973, and the Ph.D. degree in radio physics and D.Sc. (habilitation) degree in physical electronics from the Kotel'nikov Institute of Radio Engineering and Electronics, Russian Academy of Sciences, Moscow, in 1978 and 1990, respectively.

Since 1973, he has been with the Kotel'nikov Institute of Radio Engineering and Electronics, Russian Academy of Sciences, where he is currently the Head of the Laboratory of superconducting devices for signal detection and processing.

S. F. Likhachev, photograph and biography not available at the time of publication.

Authorized licensed use limited to: Kotel'nikov Inst of Radio Eng & Electronics - RAS. Downloaded on April 18,2025 at 13:46:57 UTC from IEEE Xplore. Restrictions apply.